NUMERICAL STUDY ON ADAPTIVE WING STRUCTURE USING LEADING AND TRAILING EDGE FLAPS FOR REDUCTION OF BENDING MOMENT

Kanata FUJII[+1], Tomohiro YOKOZEKI[+2], Hitoshi ARIZONO[+3] and Masato TAMAYAMA[+4]

[+1, +2]The University of Tokyo, Tokyo, Japan

[+3, +4]Japan Aerospace Exploration Agency, Tokyo, Japan

Recent commercial aircraft have high aspect ratio wings to improve the fuel efficiency. However, it is concerned that the margin of wing strength gets smaller, especially at the wing root. In order to deal with the problem, adaptive wing structure, which can change the lift-to-drag ratio in flight, is considered. By using the adaptive wing structure, the lift distribution can be modified so that the bending moment decreases. The purpose of this paper is to investigate the effectiveness of adaptive wing structure for reducing the bending moment and the stress. For this purpose, static aeroelastic analysis is conducted with a semispan wing model using MSC/NASTRAN. The model is composed of spars, ribs and skins, and has 4 flaps at each of its leading and trailing edges. The set of flap deflection angles is optimized to minimize the wing root bending moment in a 2.5 pull-up maneuver with Response Surface Methodology (RSM) using MATLAB. As a result, the wing root bending moment is successfully reduced by 10~35% in comparison to that of the original configuration whose flaps have 0° deflection angles.

Keyword: Adaptive wing, Aeroelasticity, Optimization, Response surface methodology

1. INTRODUCTION

　　　With recent emphasis on the environmental feasibility, the demand for fuel efficient aircraft is increasing. These aircraft have some features to reduce the fuel consumption and to improve the fuel efficiency. One of the remarkable features of these aircraft is to introduce lightweight materials, such as carbon fiber reinforced plastics, to reduce the total weight. Another remarkable feature is to introduce a high aspect ratio wing to reduce the induced drag. Many of today's commercial aircraft have high aspect ratio wing on the order of 10, and the future aircraft concept proposed by Boeing and NASA has that of about 20[1]. The wing aspect ratio is expected to increase. However, such a high aspect ratio wing usually shows the decrease of its stiffness and the increase of wing root bending moment, and causes the deterioration of wing strength performance. Especially, the wing root bending moment is the most serious when the aircraft is in high g maneuver or in the condition encountering gust. One of the solutions to improve wing strength is to add some structural members, such as strut. These members support a part of the wing load and reduce the load applied on the wing. However, these members make the drag and the weight larger, and this results in the decrease of fuel efficiency. In order to deal with this problem without the increase of drag or weight, an adaptive wing structure is considered.

　　　Adaptive wing structure is the structure whose wing can change the camber and the lift-to-drag ratio in flight. The typical constitution of this wing has variable camber surfaces at its leading and trailing edges. Here, the variable camber surfaces refer to control surfaces such as flaps, ailerons and other discontinuous surfaces although Powers et al. permit only smooth surfaces[2]. By introducing adaptive wing structure, the wing can change its spanwise distribution of camber, and also, the spanwise distribution of lift can be controlled. This controllability of lift distribution is the best merit of adaptive wing structure. Generally, aircraft's wings are designed to be either optimal for a single cruise flight condition or near-optimal for multiple flight conditions, that is, the wings are less optimal for any other flight conditions[3]. Adaptive wing can modify the spanwise lift distribution in flight to be more suitable for wider condition in flight profile. Several previous studies have been conducted to investigate the potential performance of adaptive wing structure for drag reduction[2-7] or load

[+1]fujii@aastr.t.u-tokyo.ac.jp, [+2]yokozeki@aastr.t.u-tokyo.ac.jp, [+3]arizono.hitoshi@jaxa.jp, [+4]masato@chofu.jaxa.jp

alleviation[8, 10]. Rodriguez et al. conducted aeroelastic analysis of a wing of Generic Transport Model (GTM) aircraft with the adaptive wing which is known as the Variable Camber Continuous Trailing Edge Flap (VCCTEF), and showed the wave drag reduction[3]. Lebofsky et al. showed the large reduction of the bending moment of the Truss-Braced Wing (TBW) by deflecting the VCCTEF[8]. Tamayama et al. also applied adaptive wing to High Altitude Long Endurance Aerial Vehicle (HALE) whose wing aspect ratio is about 20, and large amount of wing root bending moment was reduced[10]. By using this adaptive wing, it is possible to concentrate the lift on the inboard wing so that the bending moment decreases.

The purpose of this paper is to investigate the effectiveness of the adaptive wing structure for reducing bending moment and stress by controlling the spanwise lift distribution. For this purpose, static aeroelastic analysis is conducted using the semispan wing model based on the 120-passenger commercial transport aircraft[11] with SOL144 solver in MSC NASTRAN. The wing model has 4 flaps which can be deflected independently at each of its leading and trailing edges. To improve the fidelity, the wing model is composed of spars, ribs and skins in this study; many of previous researches treated the wing as bars or plates. The particular flight condition under the consideration is a 2.5g pull-up maneuver. The set of flap deflection angles is optimized to minimize the bending moment at the wing root with Response Surface Methodology (RSM) using MATLAB.

2. ANALYSIS

In this paper, aeroelastic analysis is conducted to consider the change of aerodynamic force generated by the wing deformation. To perform aeroelastic analysis, two analysis models are needed: one is structural model and another is aerodynamic model. These two analysis models and the analysis conditions are explained in this section.

(1) Analysis model

The semispan wing model is based on the 120-passenger commercial transport aircraft JAXA Technology Reference Aircraft (TRA) 2012A[11]. The specification of the JAXA TRA2012A is shown in Tab. 1. By using the values in Tab.1, the semispan wing model is generated and its two-view drawing is shown in Fig. 1. Here, the swept-back angle at 25% chord line and the dihedral angle are assumed to be both 0°, and taper ratio is set to be 0.3. The root and tip chord lengths are 5.13 m and 1.66 m, respectively. The semispan length is 15.2 m. The wing thickness at root and tip are 0.718 m and 0.234 m, respectively. The chord length and the wing thickness vary linearly along the spanwise direction. There are 4 flaps whose spanwise length are equally 3.8 m at each of the wing leading and trailing edges as devices to modify the spanwise lift distribution. The leading- and trailing-edge flaps are tagged as "LEF i" and "TEF i" respectively: here i=1~4 and "i" is the flap number counting from the most inboard one. Finite Element Analysis (FEA) model is shown in Fig. 2. The wing model is composed of spars, ribs and skins in order to investigate the stress of each member, though many of previous researches treated the wing as bars or plates in their structural model. In Fig. 2 the skins at Flap 3 and 4 are removed so that it is easy to see the inner structure. A geometrical gap exists between each of LEFs and TEFs and wing box in structural model; there are no gaps in aerodynamic model. The wing section has the super critical airfoil NASA/Langley SC (2)-0714[12]. The front and rear spars are placed at 15% and 60% chord line from leading edge, and each flap section has 7 ribs. The FEA nodes are generated by dividing the wing into 25 elements in chordwise direction and 96 elements in spanwise direction. The elements used in the FEA model

Table 1: Specification of JAXA TRA2012A.

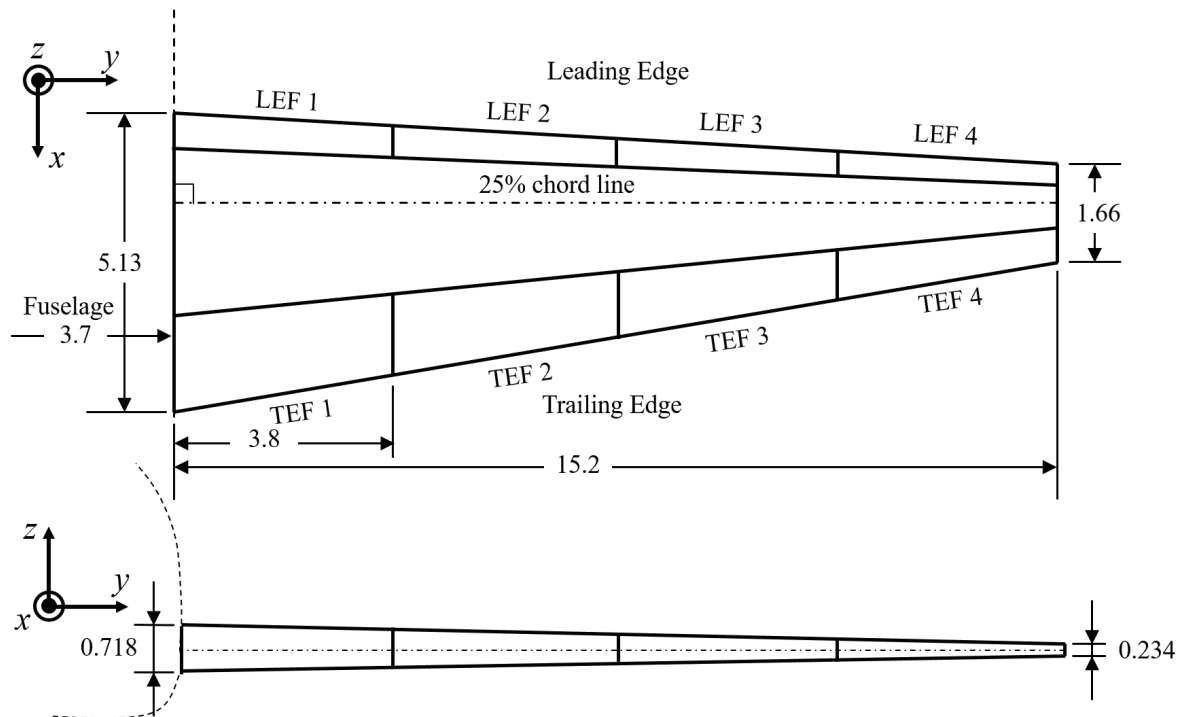| Cruise Mach Number	0.78
Wing Area	122.4 m^2
Aspect Ratio, AR	9.5
Fuselage Diameter	3.7 m
Coefficient of Lift at Cruise, C$_L$	0.5194

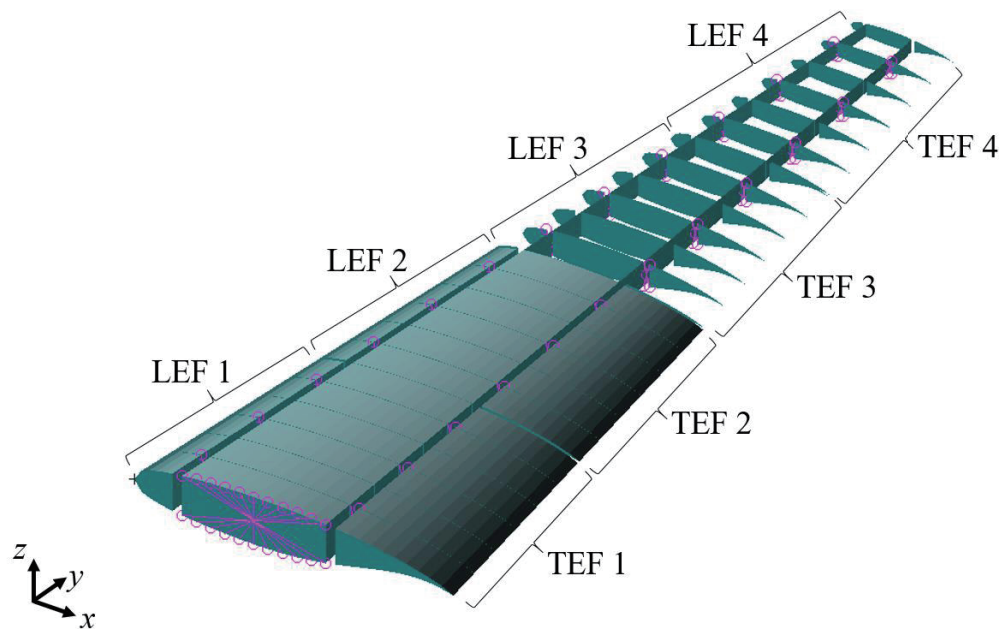Figure 1: Two-view drawing of wing model (unit: m).

Figure 2: Finite element analysis model.

are shell elements (CTRIA3 or CQUAD4 in MSC Nastran) with 3 or 4 nodes. The material of the structure is assumed ultra-duralumin. The thicknesses of each member at root and tip are shown in Tab. 2, and those vary linearly along the wing span. The flaps are attached to the wing box with rigid bar elements placed at the 2nd, 4th and 6th ribs of each flap counting from inboard. The wing model is constrained rigidly at the wing root with

the node placed at the center of the wing root which are connected to all of the nodes of wing box at root with the constraint having 6 degrees of freedom.

The aerodynamic model is shown in Fig. 3. The wing is divided into 10 panels in chordwise direction and 40 panels in spanwise direction. In SOL144 solver of MSC NASTRAN, all lifting surfaces are assumed to be the panels lying nearly parallel to the flow, and camber is included as a downwash of each panel.

(2) Analysis conditions

The particular flight condition considered in this study is a 2.5g pull-up maneuver. The cruise mach number is 0.78 from Tab. 1 and the cruise altitude is assumed to be 35,000 ft; and then the cruise speed, V_c, is 231.2 m/s. The load factor n is assumed to be 2.5. The Angle Of Attack (AOA) is set to be 7.6° so that the wing generates 2.5 times as large lift as that of cruise condition at the speed V_c without any flap deflections. This case is taken as the baseline in this study and is called as "base condition". The gross lift, wing root bending moment and maximum von-Mises stress of spars, ribs and skins of the base condition are presented in Tab.3.

Table 2: Thicknesses of spars, ribs and skins [mm].

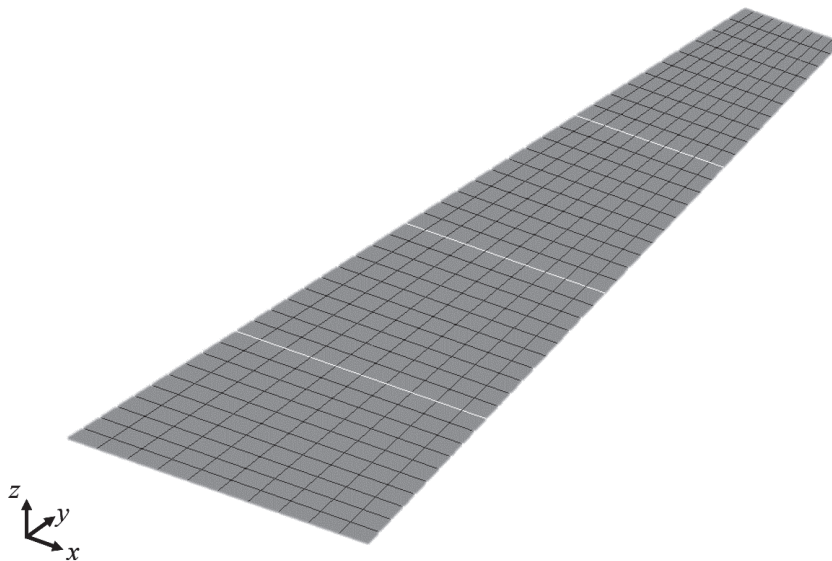|		Root	Tip
Spar		5.0	3.0
Rib		4.0	2.0
Skin	Wing Box	12.0	4.0
	Flap	4.0	2.0

Figure 3. Aerodynamic model.

Table 3: Gross lift, wing root bending moment and maximum von-Mises stress of the base condition.

Gross Lift, L_0 [N]		8.086×10^5
Wing Root Bending Moment [Nm]		5.087×10^6
Maximum von-Mises Stress [N/m^2]	Spars	1.740×10^8
	Ribs	5.884×10^7
	Skins	3.006×10^8

3. OPTIMIZATION OF A SET OF FLAP DEFLECTION ANGLES

(1) Response Surface Methodology [13]

In this paper, many design parameters are used to minimize the wing root bending moment. To get more precise result, all sets of flap deflection angles should be analyzed; however, it is not realistic because it takes much calculation cost. Therefore, Response Surface Methodology (RSM) is used to approximate the relationship between design parameters and a response of interest, and to reduce the calculation cost. In general, response y can be expressed as a function of design parameters, $x_1, x_2, ..., x_k$, by a low-degree polynomial model as follows.

$$y = \beta_0 + \sum_{i=1}^{k} \beta_i x_i + \sum_{i<j} \beta_{ij} x_i x_j + \sum_{i=1}^{k} \beta_{ii} x_i^2 + \varepsilon \tag{1}$$

Here, the second-degree model is chosen. βs (β_i, β_{ij}, β_{ii}) are unknown constant coefficients and ε is a error. In order to determine the coefficients βs, a series of experiments should be carried out, and the number of experiments is determined by central composite design: the design of experiments which is usually used for second-degree model. In this study, the lift and the wing root bending moment are approximated as functions of flap deflection angles.

(2) Design parameters

The design parameters for the optimization problem are flap deflection angles.

$$\boldsymbol{\delta} = \{\delta_{\text{LEF1}}, \delta_{\text{LEF2}}, \delta_{\text{LEF3}}, \delta_{\text{LEF4}}, \delta_{\text{TEF1}}, \delta_{\text{TEF2}}, \delta_{\text{TEF3}}, \delta_{\text{TEF4}}\} \tag{2}$$

$\delta_{\text{LEF}i}$ and $\delta_{\text{TEF}i}$ are flap deflection angles of LEF i and TEF i, respectively. Fig. 4 shows the definition of flap angle sign. Nose-up is positive for the LEFs and nose-down is positive for TEFs.

(3) Objective function

For the cantilever wing in a 2.5g pull-up maneuver, the maximum spanwise bending moment occurs at the wing root. Reducing the maximum bending moment also causes the reduction of bending moment at other parts. Therefore, the objective function is the wing root bending moment ($M_{\text{root}}(\boldsymbol{\delta})$, a function of $\boldsymbol{\delta}$), and the optimization analysis is conducted to find $\boldsymbol{\delta}$ to attain minimum $M_{\text{root}}(\boldsymbol{\delta})$. Here, the wing root bending moment $M_{\text{root}}(\boldsymbol{\delta})$ is positive when the wing deformation curve shows its center of curvature beyond the wing upper surface.

(4) Constraints

If there were no constraints in this optimization problem, the result would be unrealistic, such as a result whose gross lift is 0. Therefore, the minimization problem is subjected to several constraints. First of all, the upper and lower limit, $\delta_{\max}$, should be applied to δs (δ_{LEF}, δ_{TEF}), that is $-\delta_{\max} \leq \delta s \leq \delta_{\max}$. This limitation is required to avoid reaching the results which include extremely large angle values. Four cases of $\delta_{\max}$, 5°, 10°, 15° and 20°, are considered. Next, in order to maintain the flight condition, the gross lift $L(\boldsymbol{\delta})$ is made to be

Figure 4: Definition of flap angle sign (i=1~4).

equal to and not to be less than the base condition value of L_0=8.086×10^5 N, that is $0 \leq (L(\boldsymbol{\delta})-L_0)/L_0 \leq 0.01$. The summary of the objective function and constraints is as follows.

$$\min_{\boldsymbol{\delta}} M_{\text{root}}(\boldsymbol{\delta}) \text{ such that } \begin{cases} -\delta_{\max} \leq \delta s \leq \delta_{\max} \ (\delta_{\max} = 5°, 10°, 15°, 20°) \\ 0 \leq \dfrac{L(\boldsymbol{\delta}) - L_0}{L_0} \leq 0.01 \end{cases} \tag{3}$$

The bending moment $M_{\text{root}}(\boldsymbol{\delta})$ and gross lift $L(\boldsymbol{\delta})$ are approximated by Response Surface Methodology (RSM).

4. RESULTS & DISCUSSIONS

The optimization under the conditions presented by Eq. (3) was conducted. The optimized sets of flap deflection angles are shown in Fig. 5 and Tab. 4. Regardless of the value of $\delta_{\max}$, flaps are similarly deflected as the inboard lift to increase and the outboard lift to decrease.
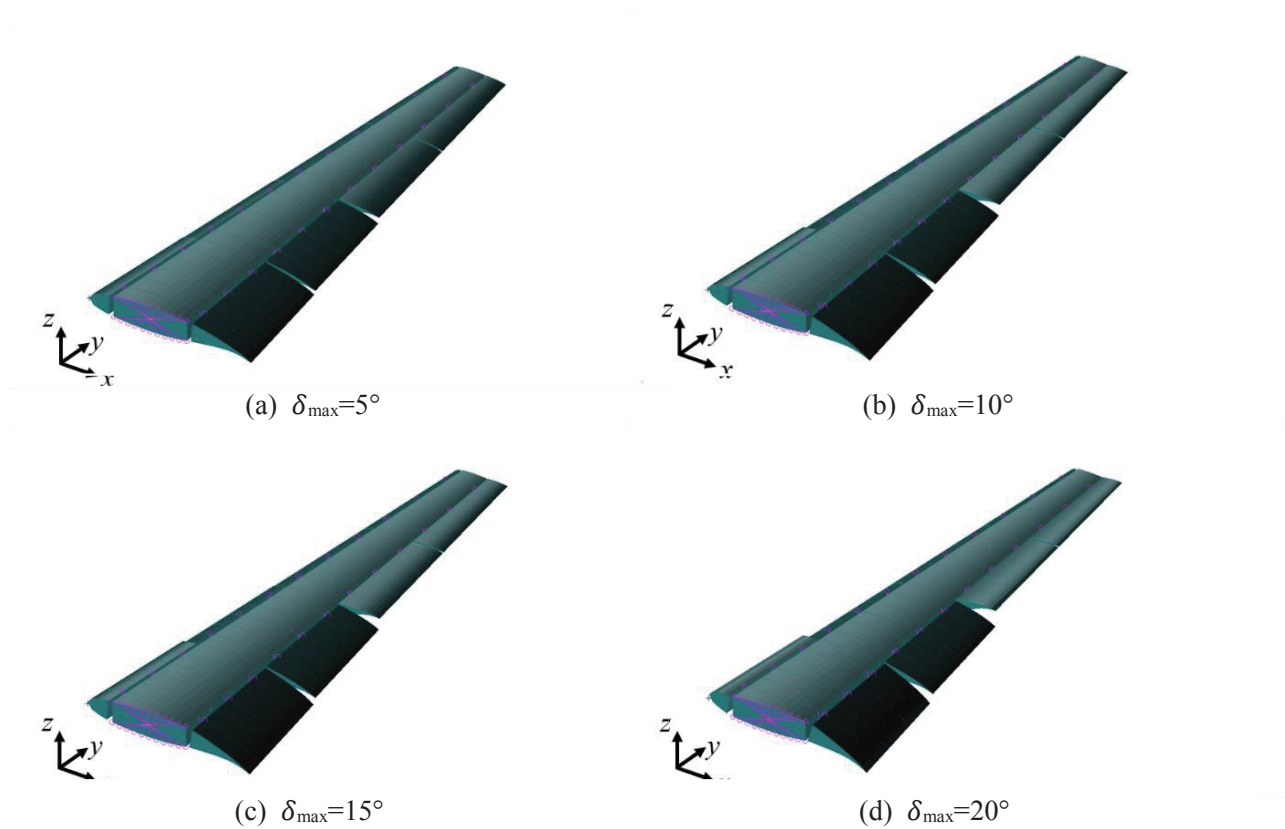

(a) $\delta_{\max}$=5°   (b) $\delta_{\max}$=10°

(c) $\delta_{\max}$=15°   (d) $\delta_{\max}$=20°

Figure 5: Optimized flap deflections.

Table 4: Optimized set of flap deflection angles [°].

$\delta_{\max}$	δ_{LEF1}	δ_{LEF2}	δ_{LEF3}	δ_{LEF4}	δ_{TEF1}	δ_{TEF2}	δ_{TEF3}	δ_{TEF4}
5	1.0	-1.9	-5.0	-5.0	5.0	1.8	-5.0	-5.0
10	4.2	-7.0	-10.0	-10.0	10.0	3.5	-10.0	-10.0
15	10.7	-15.0	-15.0	-15.0	15.0	4.8	-15.0	-15.0
20	20.0	-20.0	-20.0	-20.0	20.0	4.6	-20.0	-20.0

Static aeroelastic analysis was conducted with the optimized sets of flap deflection angles using MSC NASTRAN. The spanwise lift and bending moment distributions are shown in Fig. 6 and Fig. 7 respectively. In Fig. 6, the lift generated on the inboard wing increases and that generated on the outboard wing decreases in comparison to that of the base condition. The larger δ_{max} is, the larger the lift deviation from that of the base condition is. Therefore, the bending moment decreases not only at the wing root but also along the wing span as δ_{max} increases as shown in Fig.7. The wing root bending moments M_{root} obtained from RSM and MSC NASTRAN are shown in Tab. 5, the M_{root} reducing rates of base condition for the NASTRAN result are also presented in Tab. 5. The M_{root} are well approximated by RSM. As a result, the M_{root} is reduced by 10~35%.
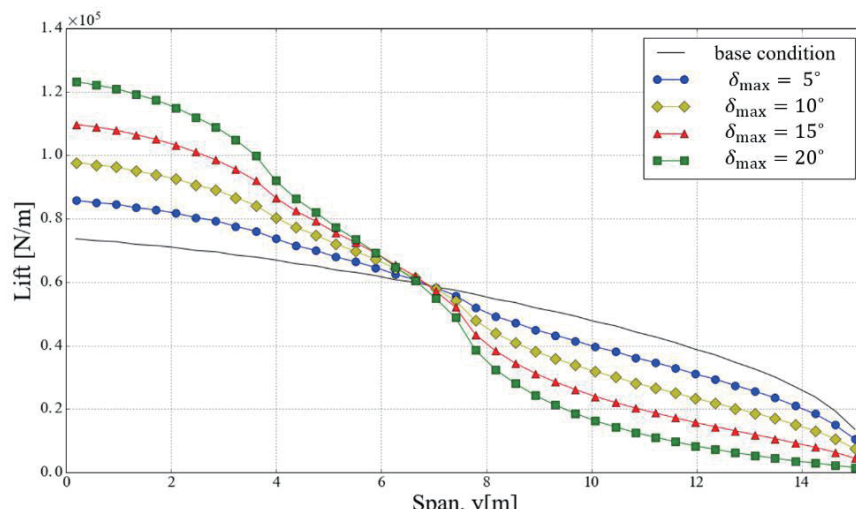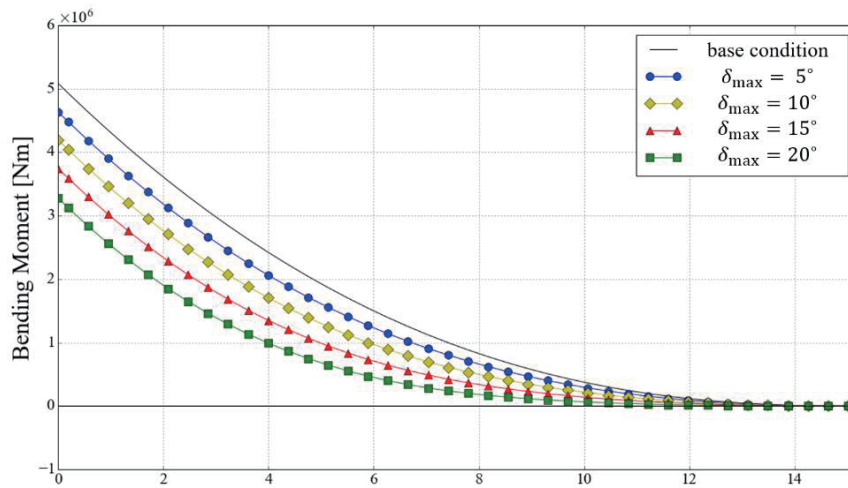

Figure 6: Optimized lift distribution.

Figure 7: Optimized bending moment distribution.

Table 5: Wing root bending moment obtained from RSM and NASTRAN, and reducing rate.

δ_{max} [°]	RSM [$\times 10^6$ Nm]	MSC NASTRAN [$\times 10^6$ Nm]	Reducing Rate (Nastran) [%]
5	4.635	4.637	-8.8
10	4.187	4.196	-17.5
15	3.746	3.746	-26.4
20	3.291	3.279	-35.5

The von-Mises stress distribution of each case is shown in Fig. 8. The high stress area, which locates in the wing box for the base condition, moves to the vicinity of wing root as δ_{max} increases. This is caused by the bending moment decrease owing to the flap deflection. The maximum von-Mises stress in each of spars, ribs and skins is plotted in Fig. 9. The maximum stress in skins decreases while that in each of spars and ribs increases as δ_{max} increases. This is caused by the increase of torsional moment. However, overall maximum stress decrease from that of base condition.

(a) base condition

(b) δ_{max}=5°

(c) δ_{max}=10°

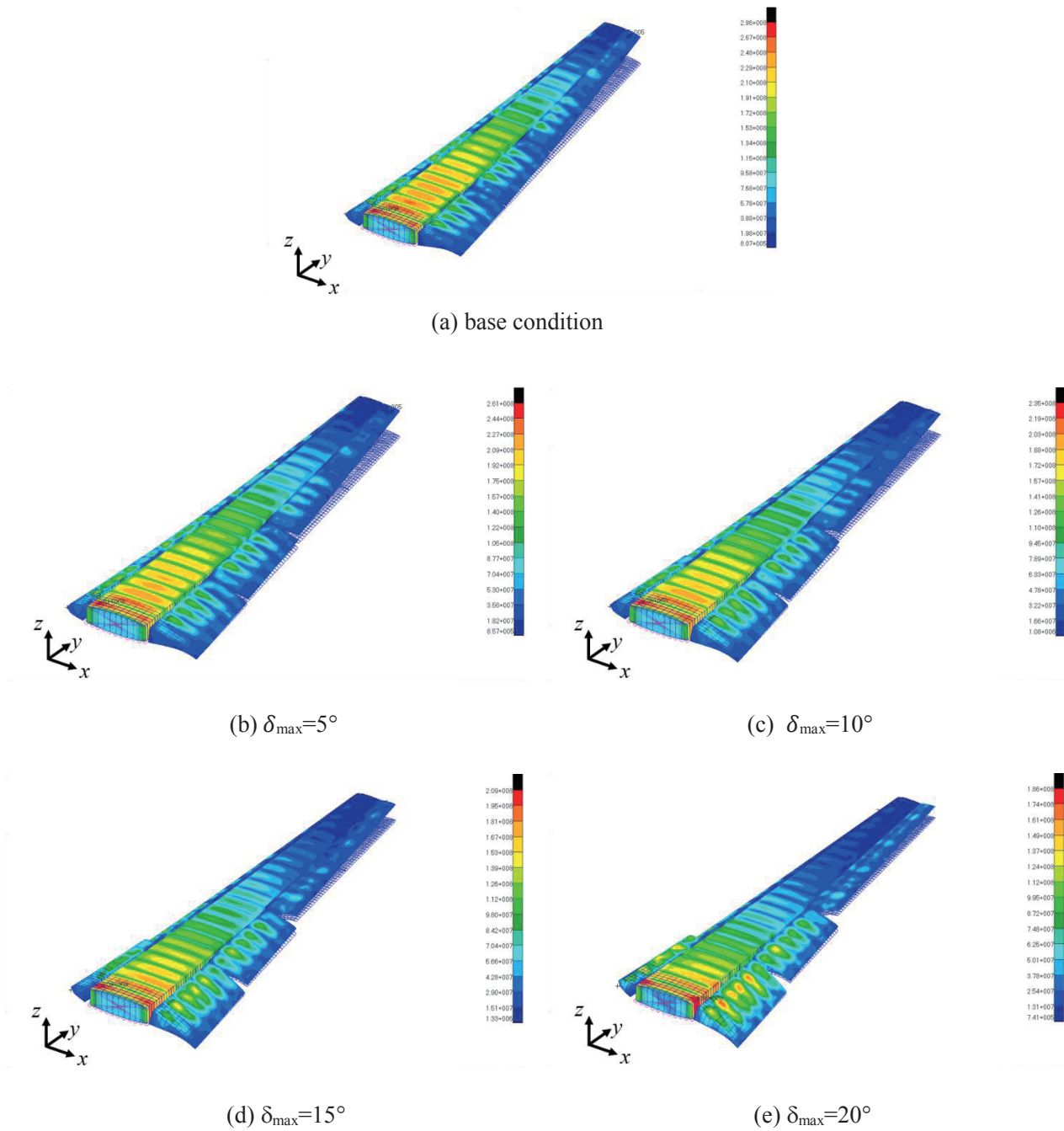(d) δ_{max}=15°

(e) δ_{max}=20°

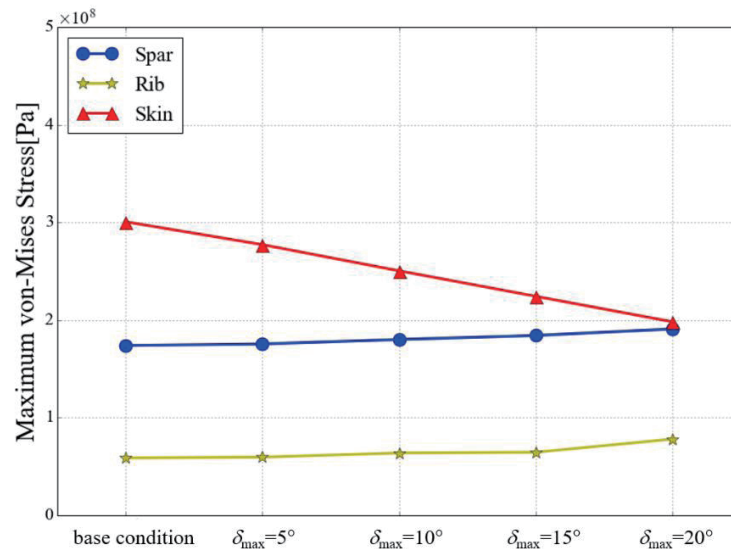Figure 8: von-Mises stress distributions.

Figure 9: Maximum von-Mises stress of spars, ribs and skins of each case.

5. CONCLUSION

In order to reduce the wing bending moment of commercial transport aircraft, the adaptive wing structure which had 4 flaps at its leading and trailing edges was considered. Static aeroelastic analysis was conducted using semispan wing model composed of spars, ribs and skins with MSC NASTRAN, and a set of flap deflection angles was optimized to minimize the wing root bending moment by using the response surface methodology. As a result, the wing root bending moment was successfully reduced by 10~35% in comparison to that of the base condition. The maximum stress was also reduced from that of the base condition, and therefore the potential effectiveness has been shown as the adaptive wing structure can make the margin of wing strength larger. As the future works, it is needed to consider drag, weight and stall to evaluate the practical importance of adaptive wing structure.

REFERENCES

1) Bradley, M. K., Droney, C. K. and Allen, T. J. : Subsonic Ultra Green Aircraft Research: Phase II –Volume I– Truss Braced Wing Design Exploration, NASA/CR-2015-218704, 2015.
2) Powers, S. G., Webb, L. D., Friend, E. L. and Lokos, W. A. : Flight Test Results From a Supercritical Mission Adaptive Wing With Smooth Variable Camber, NASA Technical Memorandum 4415, 1992.
3) Rodriguez, D. L., Aftosmis, M. J., Nemec, M. and Anderson, G. R. : Optimized Off-Design Performance of Flexible Wings with Continuous Trailing-Edge Flaps, AIAA-2015-1409, 2015.
4) Zink, P. S., Love, M. H. and Youngren, H. : Drag Minimization Through the Use of Mission Adaptive Trailing Edge Flaps and Fuel State Control, AIAA-2004-4365, 2004.
5) Nguyen, N., Precup, N., Urnes, J. Sr., Nelson, C., Lebofsky, S., Ting, E. and Livne, E. : Experimental Investigation of a Flexible Wing with a Variable Camber Continuous Trailing Edge Flap Design, AIAA-2014-2441, 2014.
6) Precup, N., Mor, M. and Livne, E. : Design, Construction, and Tests of an Aeroelastic Wind Tunnel Model of a Variable Camber Continuous Trailing Edge Flap (VCCTEF) Concept Wing, AIAA-2014-2442, 2014.
7) Nguyen, N. and Tal, E. : A Multi-Objective Flight Control Approach for Performance Adaptive Aeroelastic Wing, AIAA-2015-1843, 2015.
8) Lebofsky, S., Ting, E., Nguyen, N. and Trinh, K. : Optimization for Load Alleviation of Truss-Braced Wing Aircraft With Variable Camber Continuous Trailing Edge Flap, AIAA-2015-2723, 2015.
9) Xu, J. and Kroo, I. : Aircraft Design with Maneuver and Gust Load Alleviation, AIAA-2011-3180, 2011.

10) Tamayama, M., Fujii, K., Arizono, H. and Yokozeki, T. : Bending Moment Reduction of a High Aspect Ratio Wing, ICAST2015#32, 26th International Conference on Adaptive Structures and Technologies, 2015.

11) Kwak, D., Tamayama, M., Nomura, T. and Arizono, H. : Preliminary Studies on the Lift Distribution and Aspect ratio of Subsonic Aircraft Wing for Fuel Consumption Reduction, 3A12, 53rd Aircraft Symposium, 2015.

12) UIUC Airfoil Coordinate Database, http://m-selig.ae.illinois.edu/ads/coord_database.html.

13) Khuri, A., I. and Mukhopadhyay, S. : Response surface methodology, *WIREs Computational Statistics*, Vol. 2, pp. 128-149, 2010.